The EMBO Journal Vol. 21 No. 13 pp. 3296–3306, 2002

Involvement of the mitogen-activated protein kinase SIMK in regulation of root hair tip growth

Jozef Šamaj[1,2], Miroslav Ovecka[1,3,4], Andrej Hlavacka[3], Fatma Lecourieux[1], Irute Meskiene[1], Irene Lichtscheidl[5], Peter Lenart[1], Ján Salaj[2], Dieter Volkmann[3], László Bögre[6], František Baluška[3,4] and Heribert Hirt[1,7]

[1]Institute of Microbiology and Genetics, Vienna Biocenter, University of Vienna, Dr Bohrgasse 9, A-1030 Vienna, [5]Institut of Ecology, University of Vienna, Althanstrasse 14, A-1091 Vienna, Austria, [3]Institute of Botany, Plant Cell Biology Department, University of Bonn, Kirschallee 1, D-53115 Bonn, Germany, [2]Institute of Plant Genetics and Biotechnology, Slovak Academy of Sciences, Akademická 2, PO Box 39A, SK-950 07 Nitra, [4]Institute of Botany, Slovak Academy of Sciences, Dúbravská cesta 14, SK-842 23 Bratislava, Slovak Republic and [6]School of Biological Sciences, Royal Holloway, University of London, Egham TW20 0EX, UK

[7]Corresponding author
e-mail: hehi@univie.ac.at

Mitogen-activated protein kinases (MAPKs) are involved in stress signaling to the actin cytoskeleton in yeast and animals. We have analyzed the function of the stress-activated alfalfa MAP kinase SIMK in root hairs. In epidermal cells, SIMK is predominantly nuclear. During root hair formation, SIMK was activated and redistributed from the nucleus into growing tips of root hairs possessing dense F-actin meshworks. Actin depolymerization by latrunculin B resulted in SIMK relocation to the nucleus. Conversely, upon actin stabilization with jasplakinolide, SIMK co-localized with thick actin cables in the cytoplasm. Importantly, latrunculin B and jasplakinolide were both found to activate SIMK in a root-derived cell culture. Loss of tip-focused SIMK and actin was induced by the MAPK kinase inhibitor UO 126 and resulted in aberrant root hairs. UO 126 inhibited targeted vesicle trafficking and polarized growth of root hairs. In contrast, overexpression of gain-of-function SIMK induced rapid tip growth of root hairs and could bypass growth inhibition by UO 126. These data indicate that SIMK plays a crucial role in root hair tip growth.

Keywords: actin cytoskeleton/MAP kinase/root hairs/signaling/tip growth

Introduction

Mitogen-activated protein kinases (MAPKs), a specific class of serine/threonine protein kinases, are involved in controlling many cellular functions in all eukaryotes. A general feature of MAPK cascades is their composition of three functionally linked protein kinases. An MAPK is phosphorylated and thereby activated by a MAPK kinase (MAPKK), which itself becomes activated by another serine/threonine protein kinase, a MAPKK kinase (MAPKKK). Targets of MAPKs can be various transcription factors, protein kinases or cytoskeletal proteins (Whitmarsh and Davis, 1998).

Signaling through MAPK cascades is involved in cell differentiation, division and stress responses (Robinson and Cobb, 1997). In plants, a number of studies have demonstrated that MAPKs are signaling biotic and abiotic stresses, including cold and drought (Jonak *et al*., 1996), wounding (Seo *et al*., 1995; Bögre *et al*., 1997; Zhang and Klessig, 1998) and plant–pathogen interactions (Ligterink *et al*., 1997; Cardinale *et al*., 2000; Nühse *et al*., 2000). Moreover, plant MAPKs are also involved in cell division and hormone action (Ligterink and Hirt, 2001).

Studies in animal and yeast cells revealed distinct roles of various MAPKs such as dynamic organization of the actin cytoskeleton and polarization of cell growth (Mazzoni *et al*., 1993; Zarzov *et al*., 1996; Rousseau *et al*., 1997; Schäfer *et al*., 1998; Delley and Hall, 1999). Prominent examples of MAPKs controlling the actin cytoskeleton are the p38 kinase of animal cells and MPK1 of budding yeast. Both p38 and MPK1 are critical for polarization of the actin cytoskeleton (Mazzoni *et al*., 1993; Zarzov *et al*., 1996; Rousseau *et al*., 1997). The p38 kinase is also responsible for cell migration of animal cells (Rousseau *et al*., 1997) and MPK1 is involved in yeast cell growth (Mazzoni *et al*., 1993; Zarzov *et al*., 1996).

Recently, the stress-induced MAPK (SIMK) (Munnik *et al*., 1999) and its upstream activator SIMKK (Kiegerl *et al*., 2000) have been characterized and shown to be inducible by osmotic stress and various fungal elicitors (Cardinale *et al*., 2000). Here, we studied the function of SIMK during root hair formation. In trichoblasts, SIMK was located to peripheral spots predicting root hair outgrowth. In growing root hairs, SIMK was found at root hair tips together with F-actin meshworks. After treatment of root hairs with actin drugs and the MAPKK inhibitor UO 126 (Favata *et al*., 1998), changes in the actin cytoskeleton were correlated with changes in the subcellular localization and activity of SIMK. Moreover, overexpression of gain-of-function SIMK in transgenic plants resulted in increased root hair formation and growth. Our data suggest that SIMK plays an important role in root hair tip growth linking polar growth to MAPK signaling and the actin cytoskeleton.

Results

Tip-focused SIMK localization in growing root hairs

In situ hybridization with a SIMK antisense probe revealed that SIMK was strongly expressed in alfalfa root hairs (data not shown). The polyclonal M23 antibody was derived against the heptapeptide FNPEYQQ, correspond-

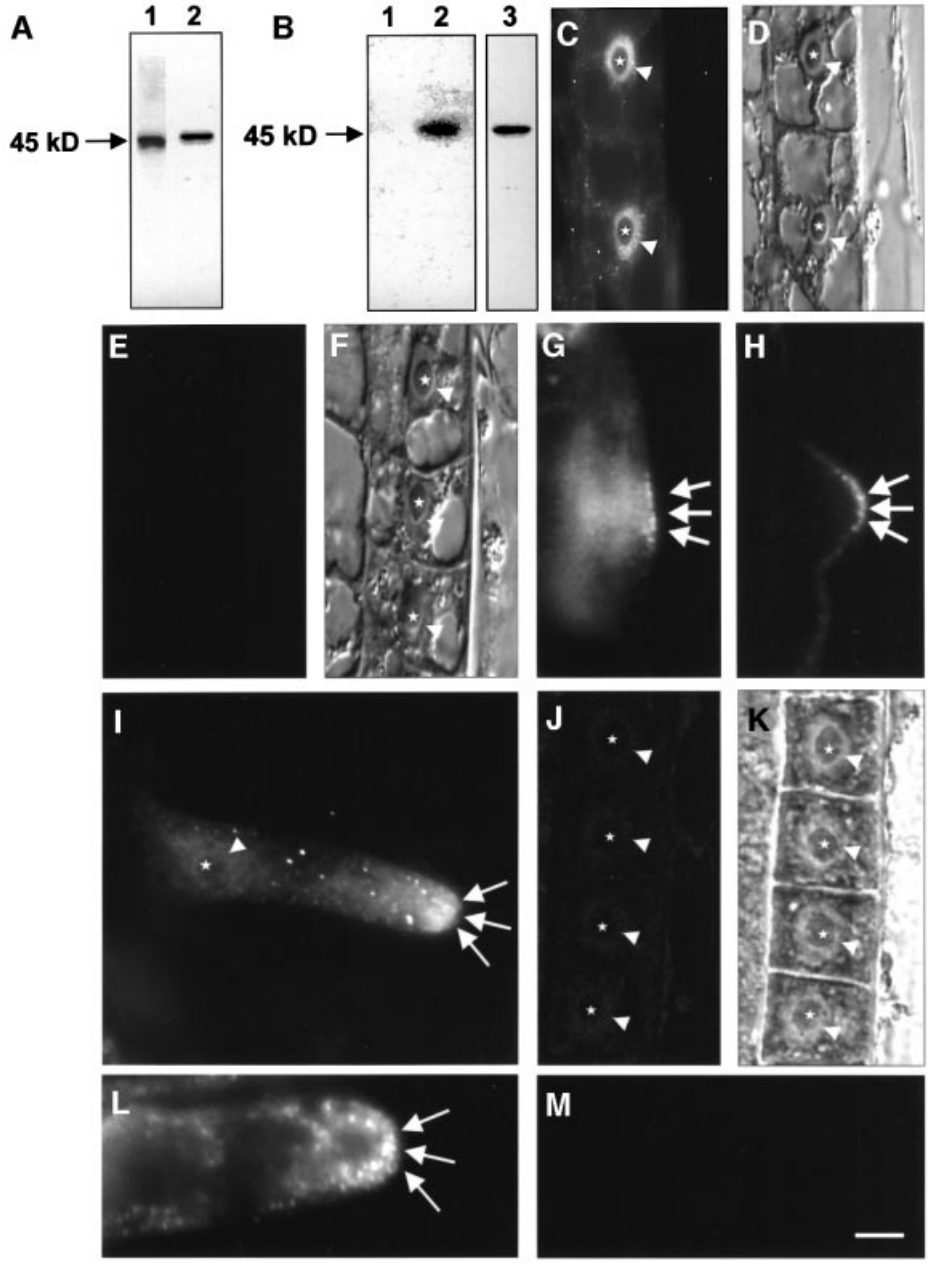

Fig. 1. Immunoblot and immunofluorescence detection of total and active SIMK. (**A**) Root extracts were prepared and immunoblotted with actin antibody (lane 1) or with SIMK antibody M23 (lane 2). (**B**) Salt treatment of roots for 10 min activated SIMK as revealed by immunoblotting crude root extracts with phospho-specific SIMK antibody N103 (lane 2) and SIMK-specific antibody M23 (lane 3). Active SIMK is hardly detected in control roots with N103 (lane 1). (**C**) Immunofluorescence microscopy of SIMK in elongating root cells of *M.sativa* L. using the Steedman's wax embedding technique. Note that SIMK is localized predominantly to nuclei (indicated by arrowheads), but depleted from nucleoli (indicated by stars). (**D**) DIC image of (C). (**E**) Immunodepletion control of epidermal root cells (shown in F) with M23 after pre-incubation with FNPEYQQ heptapeptide. (**F**) Corresponding DIC image for (E). (**G**) Trichoblast before root hair initiation showing cell periphery-associated spot-like SIMK labeling at the outer tangential cell wall (arrows). (**H**) Trichoblast at the bulging stage: SIMK labeling appears at the outermost domain of the developing bulge (arrows). (**I**) Growing root hair showing SIMK labeling focused to the tip (arrows) and in spot-like structures along the root hair tube. SIMK is depleted from the nucleus and nucleoli (arrowhead and star, respectively). (**J**) Root epidermal cells showing very low levels of active SIMK labeled with N103 antibody. (**K**) Corresponding DIC image for (J). Nuclei and nucleoli in (J) and (K) are indicated by arrowheads and stars. (**L**) Tip of a growing root hair showing accumulation of active SIMK in spot-like structures at the root hair tip (arrows). (**M**) Immunodepletion control of root hair with N103 after pre-incubation with CTDFMTpEYpVVTRWC peptide. Bar = 15 μm for (C–F), 10 μm for (G–K) and 5 μm for (L) and (M).

ing to the C-terminus of SIMK (Cardinale *et al*., 2000), and specifically recognizes SIMK but not other related MAPKs (Munnik *et al*., 1999; Cardinale *et al*., 2000). Immunoblot analysis of root extracts revealed that M23 recognized a single band of 46 kDa that corresponds to SIMK (Figure 1A, lane 2). A monoclonal actin antibody used in this study reacts specifically with a single band of 45 kDa in crude root cell extracts (Figure 2A, lane 1). A phospho-specific polyclonal antibody N103 was raised in rabbit against CTDFMTpEYpVVTRWC peptide of

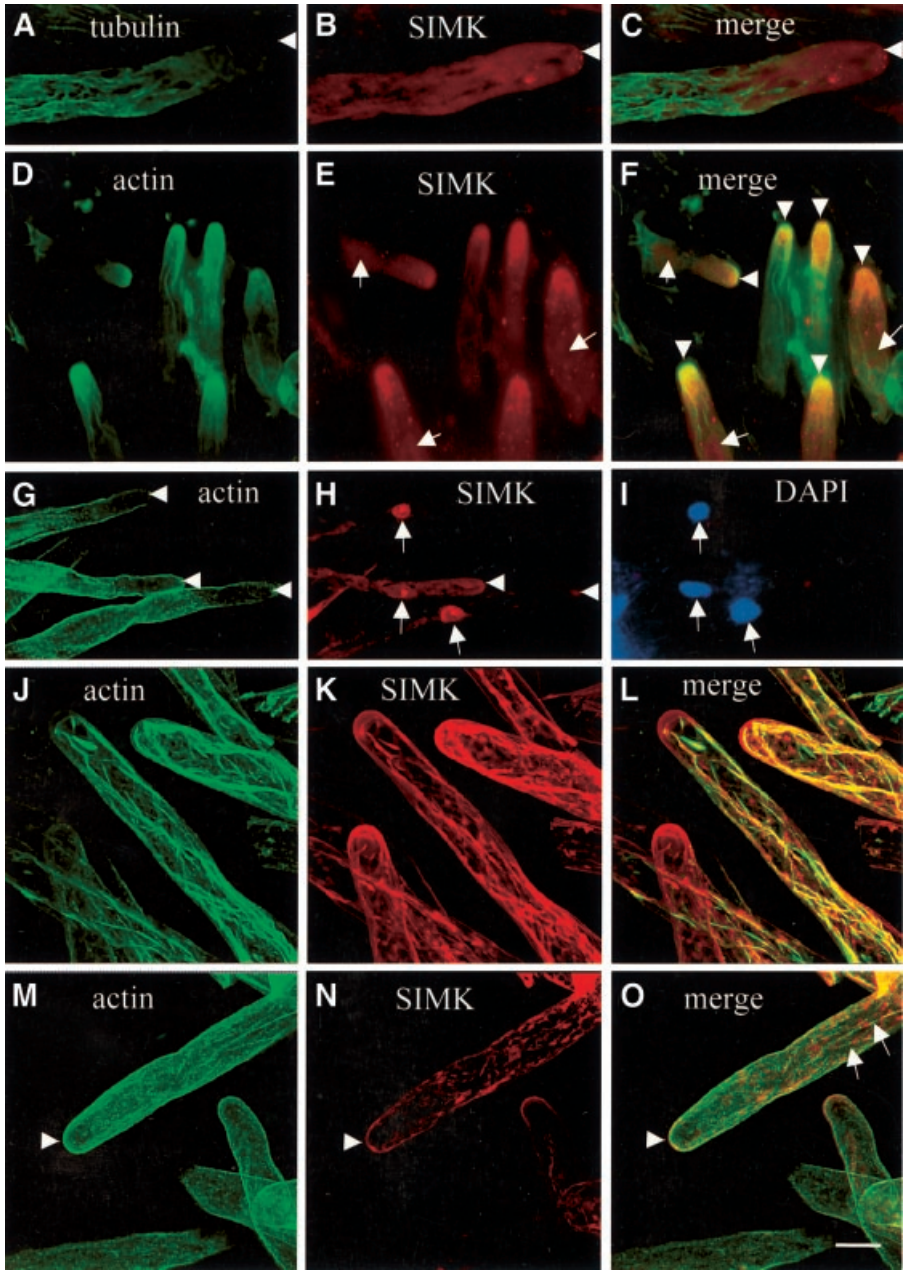

Fig. 2. Co-immunolocalization of tubulin and SIMK (A–C) or actin and SIMK (D–O) in root hairs using the freeze-shattering technique. (**A**) Microtubules are organized in longitudinal and net-axially arranged arrays in non-growing parts of the root hair tube and are much less abundant in subapical and apical zones of growing root hair apices. (**B**) SIMK accumulates in root hair apices and in distinct spots. (**C**) Merged image indicating no significant co-localization (yellow color) of microtubules and SIMK at root hair tips and within root hair tubes. Arrows indicate root hair tip. (D–F) Control growing root hairs. (G–I) Growing root hairs treated with 10 μM latrunculin B (LB) for 30 min. (J–L) Growing root hairs treated with 5 μM jasplakinolide (JK) for 60 min. (M–O) Growing root hairs treated with 50 μM brefeldin A (BFA) for 60 min. (**D**) Dense actin meshworks are present at root tips, and F-actin organizes in the form of longitudinal bundles further away from the root hair tip. (**E**) SIMK accumulation in root hair apices and in distinct spots further away from the hair tip. (**F**) Co-localization (yellow color) of actin and SIMK at root hair tips (indicated by arrowheads). Nuclei are indicated by arrows in (E) and (F). (**G**) LB disrupts F-actin in growing root hairs and depletes actin from root hair tips (arrowheads). (**H**) SIMK relocates from tips (arrowheads) to nuclei (arrows) upon LB treatment. (**I**) DAPI staining of (H). Nuclei are indicated by arrows. (**J**) JK induces F-actin stabilization and the appearance of thick actin cables protruding to root hair tips. (**K**) SIMK is located to thick cables and to round-shaped cytoplasmic spots after JK treatment. (**L**) Extensive co-localization (yellow) of SIMK with thick F-actin cables in JK-treated hairs. (**M**) BFA causes the disappearance of the F-actin meshwork from the tip (arrowhead) while F-actin filaments deeper in the cytoplasm remain intact. (**N**) SIMK is relocated from the tip and concentrates in patches within the cytoplasm in BFA-treated hairs. (**O**) SIMK patches are associated with actin filaments (arrows) in BFA-treated hairs. Bar = 25 μm for (D–F), 30 μm for (G–I) and 15 μm for (A), (B) and (J–O).

SIMK. The N103 antibody was purified on protein A and immunoaffinity columns. Because SIMK is activated by salt stress (Munnik *et al*., 1999), protein extracts prepared from salt-treated roots were immunoblotted with N103 antibody. In untreated roots, very little active SIMK was detected by N103 (Figure 1B, lane 1). Upon salt stress, N103 specifically recognized a 46 kDa band (Figure 1B, lane 2) corresponding to SIMK as detected by the specific SIMK antibody M23 (Figure 1B, lane 3). In protoplasts co-transformed with SIMK and its activator SIMKK (Kiegerl

et al., 2000), N103 specifically recognized activated SIMK (data not shown). These data show that N103 antibody is suitable for studying activated SIMK.

In root tips, SIMK is predominantly nuclear in stele and cortex tissues, but is more abundant in epidermal cells (Baluška *et al*., 2000b). Cytological analysis of longitudinal sections from the root transition and elongation zones revealed that SIMK was mostly present in nuclei of epidermal cells (arrows in Figure 1C and D). SIMK showed a spot-like nuclear staining, but was not detected in nucleoli (stars in Figure 1C). An immunodepletion control in which the SIMK antibody was pre-incubated with the FNPEYQQ heptapeptide confirmed the specificity of labeling in roots (Figure 1E and F).

When root hair formation was analyzed, SIMK was found to accumulate in outgrowing bulges and at root hair tips (Figures 1G–I and 2E). SIMK accumulated in distinct spots at the cell periphery facing the outer tangential cell wall of trichoblast (Figure 1G) marking the site of bulge outgrowth. During bulge formation, SIMK showed strong association with cell periphery-associated spots of the bulge (Figure 1H). In growing root hairs, SIMK was found to accumulate within root hair tips and in spot-like structures in the root hair tube (Figure 1I). This pattern of SIMK distribution along root hairs was confirmed by semi-quantitative measurements of fluorescence intensity (data not shown). Using phospho-specific N103 antibody, activation of SIMK was observed during root hair formation. In root epidermal cells, only very weak labeling was found (Figure 1J and K). In growing root hairs, active SIMK accumulated in root hair tips in the form of distinct spots (Figure 1L). An immunodepletion control in which the N103 antibody was pre-incubated with the CTDFMTpEYpVVTRWC peptide revealed no labeling in roots and confirmed the specificity of N103 antibody (Figure 1M). These data show that accumulation of active SIMK in root hair tips correlates with root hair formation.

SIMK co-localizes with F-actin meshworks in root hair tips and with F-actin cables after jasplakinolide treatment

Actin filaments, but not microtubules, are abundant at tips of growing root hairs (Bibikova *et al*., 1999; Braun *et al*., 1999; Miller *et al*., 1999) and are involved in root hair initiation and polar growth (Baluška *et al*., 2000a). Because SIMK can associate with mitotic but not cortical microtubules of dividing cells under certain circumstances (Baluška *et al*., 2000b), we also investigated whether SIMK co-localized with microtubules in growing root hairs. We did not find co-localization of SIMK with microtubules in root hair apices and in root hair tubes (Figure 2A–C). In order to study a possible SIMK association with actin filaments, we performed co-localization studies of actin and SIMK in growing root hairs (Figure 2D–F) and root hairs treated with actin drugs (Figure 2G–L). SIMK co-localized with the dense F-actin meshwork at root hair tips (Figure 2F, arrowheads) and in spots along longitudinal cables of actin filaments in subapical and deeper portions of growing root hairs. These data suggest that SIMK is associated with both the actin cytoskeleton and vesicular compartments in root hairs.

To gain further insight into the importance of F-actin and apical SIMK localization, roots were treated with latrunculin B (LB), an inhibitor of actin polymerization (Gibbon *et al*., 1999; Baluška *et al*., 2000a), or with jasplakinolide, an F-actin-stabilizing drug (Bubb *et al*., 2000). We performed time course experiments with these drugs followed by co-localization of actin and SIMK within bulges and root hairs. After treating roots for 30 min with LB, effective depolymerization of F-actin was observed in bulging trichoblasts. Under these conditions, SIMK disappeared from periphery-associated spots of root hair bulges and relocated to the nucleus (data not shown). In growing root hairs treated with LB, fluorescent spots presumably representing G-actin or patches of fragmented F-actin were distributed evenly over the entire length of the root hairs (Figure 2G). In root hair apices, LB treatment resulted in disintegration and depletion of dense apical F-actin meshworks (Figure 2G). The most intense SIMK labeling of LB-treated root hairs was found invariably within nuclei and nucleoli (Figure 2H), as revealed by nuclear 4′,6-diamidino-2-phenylindole (DAPI) staining (Figure 2I).

To study the association of SIMK with F-actin in more detail, root hairs were treated with jasplakinolide. Jasplakinolide-induced stabilization of F-actin was accompanied by the appearance of thick F-actin cables protruding into the extreme root hair tips (Figure 2J). In jasplakinolide-treated root hairs, SIMK co-localized extensively with these thick F-actin cables (Figure 2K and L). Besides this, SIMK was also located to individual spots within the cytoplasm (Figure 2K and L). These data suggest that drugs affecting the organization and dynamics of the F-actin cytoskeleton (the G-actin/F-actin ratio) have a direct impact on the intracellular localization of SIMK.

SIMK is associated with vesicular traffic in root hairs

Besides co-localization with tip-focused F-actin meshworks, SIMK was found in distinct spots along the entire length of the root hair (Figures 1 and 2). To investigate further the vesicle-associated localization of SIMK, we used brefeldin A (BFA) as an efficient inhibitor of vesicular trafficking in plant cells (Satiat-Jeunemaitre *et al*., 1996). Upon BFA treatment, the apical dense meshworks of F-actin in growing root hairs disappeared (Figure 2M) and SIMK was located throughout the root hair cytoplasm in spotty and patchy structures of variable sizes (Figure 2N). These BFA-induced patches were distributed along F-actin (Figure 2O), indicating that the actin cytoskeleton might be important for their formation. The tip-focused gradient of SIMK and F-actin was lost in root hairs treated with BFA (Figure 2N and O). These results suggest that vesicular trafficking is involved in the control of SIMK distribution in root hair tips.

Jasplakinolide and latrunculin B induce activation of SIMK in cultured root cells

In order to investigate a possible role for the actin cytoskeleton on SIMK activity, we tested two actin drugs for their effects on SIMK activity in root-derived suspension cultured cells. Immunokinase analysis revealed that both jasplakinolide (5 μM) and LB (10 μM) activate SIMK (Figure 3, uper panel). After treating cells with LB, SIMK

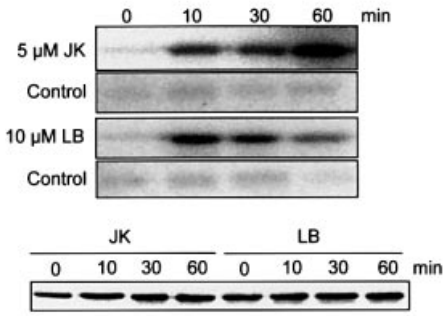

Fig. 3. Immunokinase analysis of the jasplakinolide (JK)- and the latrunculin B (LB)-induced activation of SIMK in root-derived suspension-cultured cells. Alfalfa cells were treated with 5 μM JK or 10 μM LB for the indicated times. Extracts from treated cells, containing 100 μg of total protein, were immunoprecipitated with 5 μg of protein A-purified SIMK antibody. Kinase reactions were performed with 1 mg/ml MBP as a substrate, 0.1 mM ATP and 2 μCi of [γ-^{32}P]ATP. Phosphorylation of MBP was analyzed by autoradiography after SDS–PAGE. Corresponding controls with DMSO [DMSO was used at the same concentrations as for dilution of jasplakinolide (0.25%) and latrunculin B (0.1%), respectively] showing no kinase activity at 0, 10, 30 and 60 min are presented in the lower panels. An immunoblot showing constant levels of SIMK protein during treatments with actin drugs is presented in the lowest panel.

was activated within 10 min, and activity decreased at later time points. In contrast, jasplakinolide treatment resulted in activation of SIMK after 10 min, but maximal activation was observed at 60 min. Control treatment of cells with 0.1 and 0.25% dimethylsulfoxide (DMSO), the concentrations used for applying the actin drugs, showed no SIMK activation. Importantly, SIMK protein levels were constant during treatment with both LB and jasplakinolide (Figure 3, lower panel). These data show that the state of the actin cytoskeleton affects the activity of SIMK.

Overexpression of active SIMK affects root hair formation and growth

In order to see whether SIMK is necessary for root hair growth, both gain-of-function and loss-of-function constructs of SIMK (SIMK-GOF and SIMK-LOF) were produced and stably expressed in transgenic tobacco. In analogy to the *Drosophila* rolled MAPK-GOF mutant (Brunner *et al*., 1994), the D348N exchange was introduced within the α-L16 helix in the C-terminal part of the protein. This region is involved in binding to upstream kinases and phosphatases. Transient expression assays in protoplasts showed that SIMK-GOF protein was more active than wild-type SIMK (data not shown). Biochemical analysis on stably transformed tobacco plants by M23 immunokinase assays and immunoblotting revealed that four SIMK-GOF lines showed clearly increased MAPK activity in comparison with control plants, while protein levels were similar in both control and SIMK-GOF plants (Figure 4A, upper panel). Since M23 equally recognizes SIMK and its tobacco homolog SIPK/Ntf4 (Wilson *et al*., 1998), M23 immunokinase assays determine both endogenous SIPK/Ntf4 and ectopically expressed SIMK-GOF in tobacco plants.

In a similar approach, SIMK-LOF transgenic tobacco lines were produced. The K69M point mutation within the β-3 sheet of subdomain II creates an inactive loss-of-function MAPK enzyme by disrupting the ATP-binding site (Robinson *et al*., 1996). Both in transient protoplast assays (data not shown) and in transgenic SIMK-LOF tobacco lines (Figure 4A, lower panel), no significant changes in MAPK activity and protein levels were observed.

Inspection of transgenic tobacco SIMK-GOF plants revealed that the root hair formation zone was extremely shortened and root hairs were much longer (Figure 4B) in comparison with control non-transformed roots (Figure 4C). In contrast, roots of SIMK-LOF mutant plants showed no visible root hair phenotype (Figure 4D). Taken together, these results indicate that overexpression of active SIMK stimulates root hair growth and formation.

MAPKK inhibitor UO 126 inhibits root hair growth

Since overexpression of inactive SIMK-LOF was ineffective in inhibiting root hair formation and growth, we used a MAPKK inhibitor to down-regulate MAPK activity in root hairs. For this purpose, we treated roots with UO 126, an inhibitor of MAPK activation (Favata *et al*., 1998). After a 1 h treatment, the first morphological changes in emerging and growing root hairs became evident and correlated with inhibition of root hair tip growth. After 2 h of UO 126 treatment, ballooning of emerging root hairs (Figure 5A) and swelling of apical and basal parts of growing root hairs (Figure 5D) were observed. No such effect was found using UO 124, an inactive analog of UO 126 (Figure 5B and E), or DMSO at the same concentration as a solvent for UO 126 and UO 124, respectively (Figure 5C and F). These data suggest that MAPK activity is necessary for tip growth of root hairs.

UO 126 affects actin organization and SIMK distribution within root hairs

To test whether MAPK activity is directly involved in the regulation of actin organization, roots were treated with UO 126. After UO 126 treatment, vacuolation of root hair tips (Figure 6A and B) was observed. At the same time, we noticed the partial destruction of F-actin cables located deeper within hairs and actin re-arrangement around newly formed vacuoles (Figure 6A). Under these conditions, SIMK was distributed evenly in cytoplasm and nuclei of treated hairs without any preferable accumulation in subcellular compartments (Figure 6B). In contrast, treatment with the non-active analog UO 124 caused no significant changes in tip-focused actin and SIMK localization (Figure 6C–E). These experiments indicate that inhibition of MAPK activity causes remodeling of the actin cytoskeleton in emerging root hairs.

UO 126 inhibits root hair growth by changing polar vesicular trafficking and root hair cytoarchitecture

To study the effect of UO 126-induced tip growth inhibition in root hairs in real time, we used video-enhanced microscopy. In control alfalfa root hairs, the apex (5–7 μm) was usually filled with small vesicles which were densely packed (Figure 7A) and showed random motions with a radius of 0.5–1 μm. Occasionally, several vesicles moved in a row over longer distances (3–8 μm) in the axial direction and also in various other directions

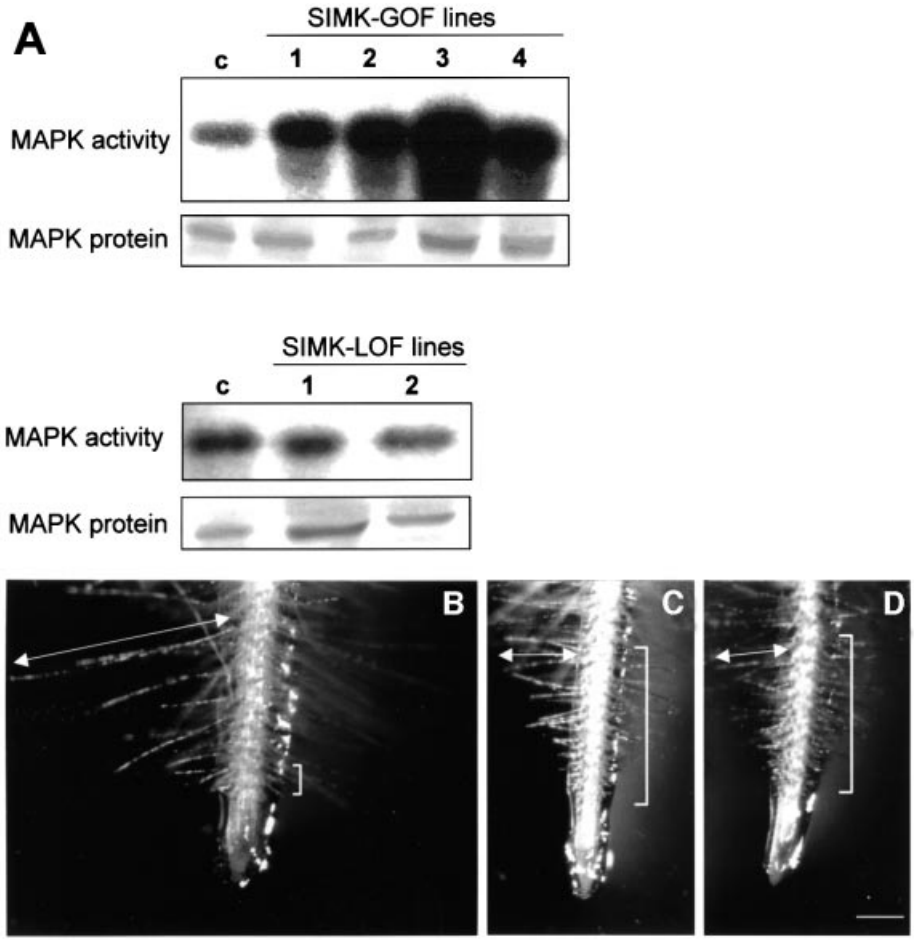

Fig. 4. Effect of overexpression of SIMK-GOF and SIMK-LOF on kinase activity and root hair formation. (**A**) MAPK activity and protein levels in control (c) tobacco SR1 plants and transformed SIMK-GOF (1–4) and SIMK-LOF (1 and 2) SR1 lines using M23 recognizing both SIMK and its tobacco homolog SIPK/Ntf4. (**B**) Root of a SIMK-GOF tobacco plant showing a very short root hair formation zone (indicated by a bracket) and much longer root hairs (indicated by arrow) as compared with (C and D). (**C** and **D**) Roots of non-transformed and SIMK-LOF plants, respectively, showing normal root hair formation zones (brackets) and regular length of root hairs (arrows). Bar = 400 μm for (B–D).

within the apical dome. Whereas large organelles were slow, vesicles moved with velocities between 4 and 6 μm/s. At the plasma membrane, secretory vesicles are supposed to fuse and deliver their contents to the cell wall, whereas endocytotic vesicles should appear at the flanks of the apical dome. These processes cannot be observed, however, due to the small size and fast movement of the vesicles.

The first signs of an effect of inhibition of MAPK activity appeared after 6–8 min of treatment with 10 μM UO 126 (Figure 7B). At this time, tip growth slowed down (from 4–6 to 1.5–2 μm/min) and finally stopped within 15 min. At 6–8 min, the movement of the vesicles became hectic and disorganized in the tip region and the amplitude of random displacements increased (1–2 μm), whereas targeted movements over longer distances disappeared (Figure 7C). Importantly, putative endocytotic vesicles at the plasma membrane became visible in cells treated with UO 126 because they stayed at apical dome flanks for 6–8 s before they disappeared (Figure 7C, H and L). In the tube, vesicles slowed down and, after 15 min, became immobile and static. Tubular small vacuoles within the tip (Figure 7D) inflated to large roundish vacuoles that oscillated in random motion (Figure 7E). Their tonoplasts were lined by vesicles and these vacuoles often fused (Figure 7E and F). During this process, the shape of the apical dome became swollen over the whole length where apical secretory vesicles showed disorganized random motions and the cell wall appeared thicker (Figure 7D–F). Similar effects of UO126 on root hair cytoarchitecture and vesicular trafficking were detected in root hairs of control tobacco plants where UO 126 caused growth arrest within 5 min (Figure 7G–I). These results suggest that UO 126 inhibits root hair tip growth by modifying cytoarchitecture and polar vesicular targeting and trafficking. Importantly, the root hairs of tobacco SIMK-GOF transgenic plants continued to grow in the presence of UO 126 (growth was inhibited by 10–15% only) and maintained root hair cytoarchitecture and normal vesicular trafficking (Figure 7J and K). In comparison with control plants, growth of SIMK-GOF root hairs was inhibited only at a 10-fold higher concentration of UO 126 (Figure 7L), showing minor changes in cytoarchitecture and no large and round vacuoles appearing in their apices (Figure 7L). These results show that overexpression of active SIMK can override inhibition of root hair growth by UO 126.

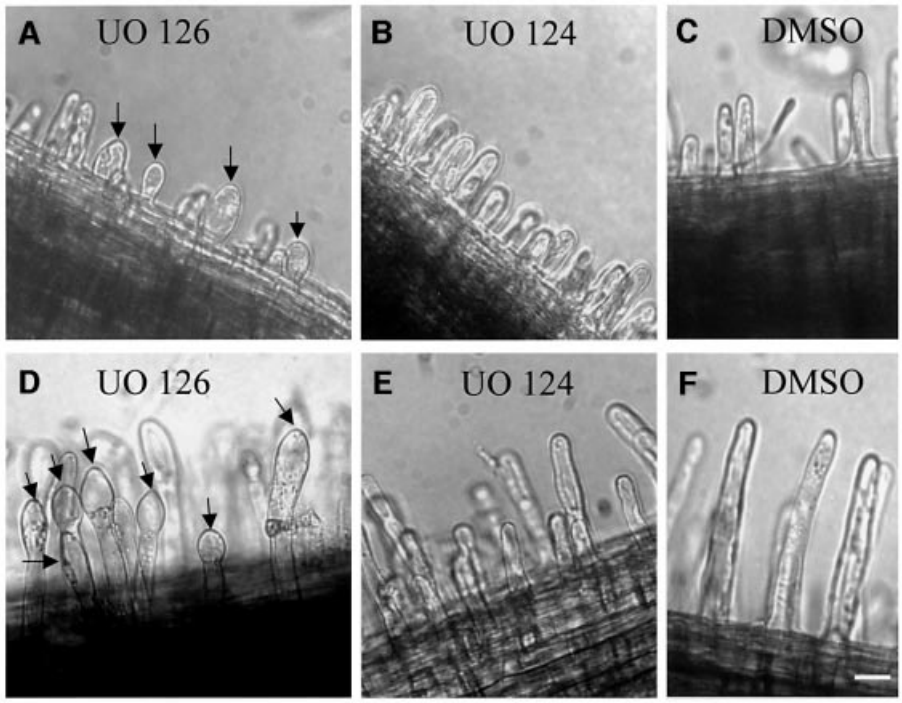

Fig. 5. Morphological changes on emerging (A) and growing root hairs (D) induced by 2 h treatment with 10 μM UO 126, a MAPKK inhibitor. (**A**) UO 126 causes swelling of emerging root hairs (arrows). (**B** and **C**) Emerging root hairs are not affected by 2 h treatment with 10 μM UO 124 or 0.1% DMSO, respectively. (**D**) UO 126 induces vacuolation and swelling of apices of growing root hairs (arrows). (**E** and **F**) UO 124 (10 μM) and (0.1%) DMSO have no morphological effect on growing root hairs. Bar = 30 μm for (A), (D) and (F), and 40 μm for (B), (C) and (E).

Discussion

The stress-activated MAP kinase SIMK is strongly expressed in root hairs. The selective enrichment of active SIMK in tips of emerging root hairs coincides with dynamic F-actin meshworks (Braun *et al*., 1999; Baluška *et al*., 2000a; Baluška and Volkmann, 2002). Depolymerization and stabilization of F-actin activates SIMK, indicating that MAPK activity is directly affected by altering F-actin dynamics. Inhibition of MAPKK activity caused changes in the subcellular distribution of actin and SIMK, resulting in tip growth inhibition and aberrant root hair morphology. Conversely, overexpression of active SIMK resulted in enhanced growth of root hairs. These data indicate that SIMK functions in root hair growth.

Active SIMK is present in root hairs

In situ hybridization and immunolocalization revealed that both SIMK transcript and protein are present within root hairs. Previously, we have shown that SIMK is localized predominantly to nuclei in meristematic cells of root apices (Baluška *et al*., 2000b). SIMK is also found in nuclei of elongating epidermal root cells (Figure 1). During bulge formation and root hair formation, SIMK is relocated polarly from nuclei towards bulging domains of trichoblasts and tips of growing root hairs, SIMK is also located at root hair tips in an active form.

MPK1 activation in yeast occurs by a weakening of the cell wall associated with stretch-stressed plasma membranes (Kamada *et al*., 1995), with concominant actin repolarization (Delley and Hall, 1999). A similar mechanism can also be envisaged for plant tip growth within outgrowing bulges and root hair tips, both representing weak cell periphery domains (Baluška *et al*., 2000a). In order to relieve the high stretch stress imposed on the plasma membrane, both abundant exocytosis (Kell and Glaser, 1993; Fricker *et al*., 2000) and dense F-actin meshworks (Ko and McCulloch, 2000) are essential,

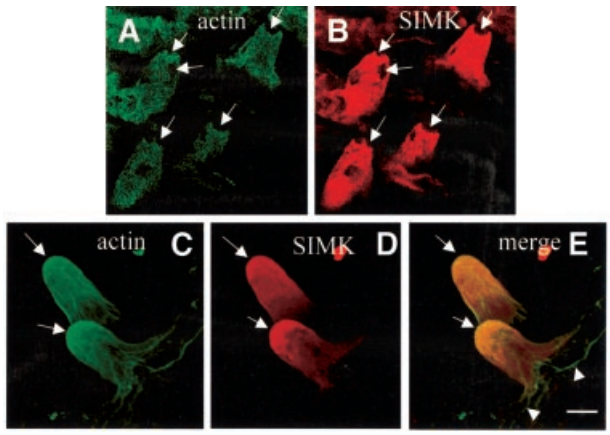

Fig. 6. Immunolocalization of actin (green, A and C) and SIMK (red, B and D) in root hairs treated with 10 μM UO 126, a MAPKK inhibitor (A and B), or with 10 μM UO 124, an inactive analog of UO 126 (C–E) for 60 min. (**A**) Note the vacuolation at the tips (arrows) and F-actin depletion from root hairs. The remaining actin labeling is evenly distributed. (**B**) SIMK is distributed evenly in root hair cytoplasm and nuclei, except holes represented by vacuoles (arrows). (**C**) The tip actin meshwork (arrows) and filamentous actin are preserved in hairs treated with UO 124. (**D**) SIMK is tip focused in hairs treated with UO 124 (arrows). (**E**) Co-localization of SIMK with actin meshworks at the tip (arrows, yellow color). Thick F-actin bundles within trichoblasts are indicated by arrowheads. Bar = 30 μm for (A) and (B), 18 μm for (C) and (D) and 23 μm for (E–G).

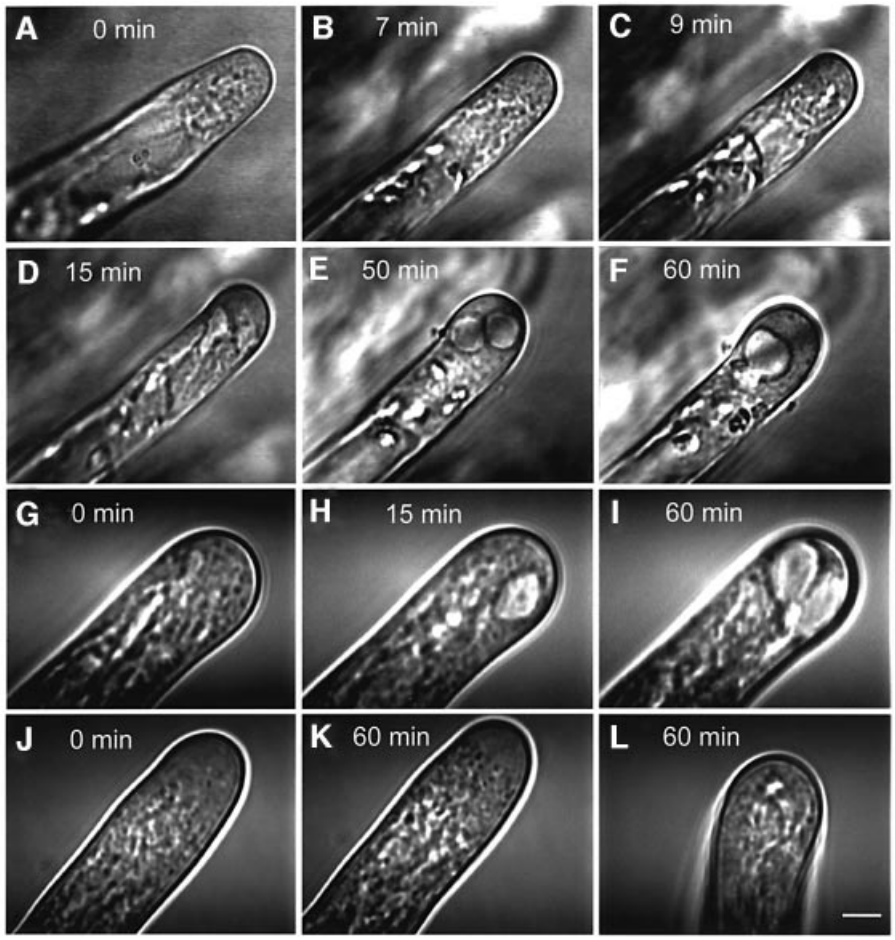

Fig. 7. Video-enhanced microscopy of growing root hairs treated with UO 126. (**A**) An untreated growing alfalfa root hair with a vesicle-rich apical dome. (**B–F**) Alfalfa root hair treated with 10 μM UO 126. Note that UO 126 markedly changes the cytoarchitecture and shape of the root hair apex causing inhibition of root hair tip growth. (**G–I**) Tobacco growing root hair treated with 10 μM UO 126. This concentration of UO 126 caused growth arrest within 5 min and similar changes in the cytoarchitecture and shape of the root hair apex to those in alfalfa (A–F). (**J–L**) Tobacco SIMK-GOF root hair treated with 10 μM UO 126 (J and K) or 100 μM UO 126 (L) for the indicated time points. Note that 10 μM UO126 did not cause growth arrest and changes in root hair cytoarchitecture and shape within 60 min, while 100 μM UO 126 inhibits root hair growth within 60 min, causing minor changes in the cytoarchitecture. Bar = 7 μm for (A–F) and 5 μm for (G–L).

culminating in the onset of root hair tip growth (Braun *et al*., 1999; Miller *et al*., 1999; Baluška *et al*., 2000a).

SIMK localization and activity are associated with actin organization

Dense F-actin meshworks at root hair tips of different plant species were observed in root hairs by immunolabeling with actin antibodies or *in vivo* using green fluorescent protein (GFP) fused to the F-actin-binding domain of talin (Braun *et al*., 1999; Baluška *et al*., 2000a; Baluška and Volkmann, 2002). An intact actin cytoskeleton is necessary for root hair tip growth because root hairs treated with the F-actin disruptors LB or cytochalasin D are inhibited in their growth and show morphological abnormalities (Miller *et al*., 1999; Baluška *et al*., 2000a; Ovecka *et al*., 2000). F-actin recruitment towards root hair bulges and growing tips roughly coincides with local accumulations of actin-depolymerizing factor (ADF) (Jiang *et al*., 1997), profilin (Braun *et al*., 1999; Baluška *et al*., 2000a) and Rop GTPases (Molendijk *et al*., 2001). SIMK was found to localize within tips of growing root hairs. Tip-focused localization of SIMK disappeared after treatment with LB and resulted in nuclear accumulation of SIMK. The association of SIMK with filamentous actin could be enhanced by jasplakinolide, an inducer of actin polymerization. These findings indicate that an intact actin cytoskeleton is necessary for the proper localization of SIMK within root hair tips. Interestingly, both actin drugs activate SIMK in suspension-cultured root cells, suggesting that the state and dynamics of the actin cytoskeleton directly influence SIMK activity. Actin reorganization is likely to be mediated by actin-binding proteins (e.g. profilin, ADF, villin, ARP, fimbrin and calponin), and SIMK might phosphorylate and regulate one of these actin-binding proteins. Both ADF and profilin are actin-binding proteins responsible for the dynamics of F-actin meshworks (for a review on plant cells see Staiger, 2000). Presently, it is not clear which actin cytoskeletal proteins are targeted by SIMK *in vivo*. In animal cells, p38 regulates the dynamic organization of the actin cytoskeleton via phosphorylation of the small heat shock protein HSP27 (Schäfer *et al*., 1998). HSP27 acts as an F-actin-capping protein inhibiting polymerization of G-actin in its phosphorylated state (Benndorf *et al*., 1994). Interestingly,

p38 is homologous to the yeast HOG1 MAP kinase that co-localizes with actin patches in osmotically stressed yeast cells (Ferrigno *et al*., 1998). Recently, it was shown that extracellular regulated kinase interacts with the actin and calponin homology domains of actin-binding proteins (Leinweber *et al*., 1999).

Our results show that SIMK is activated in response to F-actin destabilization, suggesting that SIMK might have a direct role in transmitting signals from the actin cytoskeleton to the tip growth machinery. Disturbances of actin dynamics, induced with either LB or jasplakinolide, activated SIMK. Interestingly, Gachet *et al*. (2001) reported that LB activates stress-activated MAP kinase (SAPK) of fission yeast. This F-actin-dependent SAPK cascade is part of a new mitotic checkpoint ensuring proper spindle orientation. Similarly, activation of the yeast MAP kinase MPK1 via LB-mediated depolymerization of F-actin triggers the morphogenesis checkpoint in budding yeast cells (Harrison *et al*., 2001). One possibility is that depolymerization of F-actin imposes mechanical stress on the cellular architecture which activates MAPK cascades in order to regain the balance of intracellular forces (Chicurel *et al*., 1998). This is supported by our *in vivo* observation when inhibition of MAPK activity leads to changes in cytoarchitecture and actin-dependent vesicular motilities within root hair tips. However, filamentous actin can also inhibit the activity of certain kinases, as has been shown recently for the c-Abl tyrosine kinase in mammalian cells (Woodring *et al*., 2001). This is probably not the case for SIMK in plant cells because stabilization of F-actin with jasplakinolide activates SIMK. Possibly, SIMK monitors the balance of forces, and activation of SIMK could be necessary for the recovery of a balanced cytoarchitecture (Chicurel *et al*., 1998). It would be interesting to test this idea in yeast where MAPKs monitor actin-dependent mitosis and morphogenesis checkpoints (Gachet *et al*., 2001; Harrison *et al*., 2001).

UO 126 inhibits root hair growth and disrupts polar actin and SIMK distribution

UO 126 inhibited root hair growth and affected the subcellular organization of both the actin cytoskeleton and SIMK in root hairs. As revealed by video-enhanced microscopy, the disturbance of actin-dependent polar vesicle trafficking by UO 126 is most likely responsible for the swelling and diffuse growth of root hairs.

Gain-of-function SIMK induces longer root hairs

The way in which the D334N mutation acts in the *Drosophila* MAPK rolled mutant is not well understood, but it results in a gain-of-function phenotype in the signaling pathway of *Drosophila* eye development (Brunner *et al*., 1994). Exchanging the homologous amino acid in SIMK, we observed higher MAPK activity in transformed protoplasts and plants. A possible explanation comes from analyzing a similar mutation in a yeast FUS3 allele where it was concluded that FUS3 was more active because the MAPK phosphatases were less able to inactivate the FUS3 mutant kinase (Hall *et al*., 1996). Overexpression of SIMK-GOF in tobacco plants showed a phenotype of long root hairs correlated with sustained activity of SIMK. On the other hand, overexpression of SIMK-LOF in tobacco showed no visible root hair phenotype. This result could be explained either by functional redundancy of several MAPKs in root hairs or, alternatively, by the inability of SIMK-LOF to compete sufficiently with the endogenous tobacco MAPK homolog (SIPK/Ntf4) to inhibit root hair growth. In support of functional redundancy, knockout mutants of *At*MPK6, the *Arabidopsis* homolog of SIMK, show no phenotype (K.Shinozaki, personal communication).

SIMK and vesicular traffic in root hairs

Root hairs are tubular extensions of trichoblasts growing exclusively at their tips by means of highly polarized exo- and endocytosis (Shaw *et al*., 2000). Exocytotic vesicles deliver cell wall polysaccharides such us pectins and xyloglucan (Sherrier and VandenBosch, 1994), and molecules such as lectins and arabinogalactan proteins were detected in cell walls of root hair tips (Diaz *et al*., 1989; Šamaj *et al*., 1999). On the other hand, nothing is known about endocytosis in root hairs which should be responsible for plasma membrane and cell wall recycling. By immunolocalization, active SIMK was found to accumulate in spots within root hair tips which are known to be filled with exo- and endocytotic vesicles (Sherrier and VandenBosch, 1994; this study). We show here that the MAPKK inhibitor UO 126 inhibits targeted vesicular traffic, resulting in growth arrest of root hairs. Since overexpression of SIMK-GOF in tobacco could overcome growth arrest by UO 126, it is likely that SIMK has an important function in growth control of root hairs. Because of resolution limits of video-enhanced microscopy and the dynamic behavior of abundant exocytotic vesicles, it is not possible to conclude that all exocytotic vesicles fuse to the tip plasma membrane. The vesicles could also undergo a 'kiss and run' mode of movement in delivering cell wall material to the tip. Diffuse growth and cell wall thickening at tips of UO 126-inhibited root hairs suggest that exocytosis is not blocked. On the other hand, after growth arrest with UO 126, the putative endocytotic vesicles appearing on tip flanks persist at the plasma membrane for a much longer time. These observations suggest that MAPK activity may be required for endocytosis rather than for exocytosis in growing root hairs, but clarification of this issue awaits further advances in plant endocytosis research, and future work will have to determine the exact molecular mechanism of the interdependent regulation of actin and SIMK and their roles in polar vesicular trafficking.

Materials and methods

Plant material

Seeds of *Medicago sativa* L. cv. Europa were placed on moist filter paper in Petri dishes and germinated for 3 days in cultivating chambers in darkness at 25°C. Three-day seedlings with straight primary roots 40–50 mm long were selected.

For *in vivo* observation, *M.sativa* and *Nicotiana tabacum* L. cv. SR1 (control SIMK-LOF and SIMK-GOF) seeds were sterilized and germinated on half-strength MS medium or on wet filter paper for 2 or 3 days. Seedlings were mounted between slide and coverslip that contained three layers of parafilm as spacers. Within such chambers, the primary roots could develop for at least 24 h. This method ensured that the roots could adapt to the liquid growth medium, and avoided mechanical stress during mounting of roots on the microscope. Chambers were placed upright into a Petri dish filled with Fahraeus growth medium (Fahraeus,

1957). After placing the chambers under the microscope, root hairs of short to medium length were selected and their growth was measured for at least 10 min. When elongation was normal, i.e. in the range of 0.4–0.6 μm/min, the growth medium was removed with filter paper and replaced by Fahraeus growth medium containing UO 126.

Suspension cultures were prepared from callus derived from alfalfa roots (*M.sativa* L.) and maintained as described (Baier *et al*., 1999). Log phase cells were used 3 days after a weekly 1:3 dilution in fresh medium.

Vector constructs

The SIMK-GOF mutation was created by changing D348 into N348, and the SIMK-LOF mutation was created by changing K84 into M84. Site-directed mutagenesis was performed in pALTER vector (Clontech). For recloning to plant expression vectors, PCR was performed with the following primers: SIMK 5′-*Nco*I 5′-AAAACCATGGAAGGAGGA-GGAGC-3′ and SIMK 3′-*Not*I 5′-AAAGGATCCTCAGCGGCC-GCCCTGCTGGTACTCAGGGTTAAATGC-3′.

PCR products were recloned to pBIN-HygTX vector (provided by C.Gatz, IGF Berlin) with the TMV omega leader as *Sma*I–*Xba*I inserts.

Plant transformation

Leaf discs of the SR1 tobacco line were transformed with *Agrobacterium* containing binary vector with SIMK-GOF or SIMK-LOF. Nine and four primary transformants, respectively, were regenerated from SR1 tobacco transformed with SIMK-GOF and SIMK-LOF.

Treatments with inhibitors

For dilution of drugs, distilled water or modified Fahraeus medium were used. Root apices were treated with 100 μM BFA (Sigma). LB (10 μM; Calbiochem) in 0.1% DMSO and 5 μM jasplakinolide (Molecular Probes) in 0.25% DMSO were used as actin inhibitors. For UO 126 and UO 124 inhibitors (Calbiochem), concentrations ranging from 10 nM up to 100 μM were used.

Antibodies and immunoblotting

Antibodies against SIMK (M23, recognizing the FNPEYQQ heptapeptide of SIMK) (Cardinale *et al*., 2000), phosphorylated SIMK (N103, recognizing the double-phosphorylated CTDFMTpEYpVVTRWC peptide of SIMK) and actin (clone C4, Amersham) were tested on crude root extracts as described by Bögre *et al*. (1997). Immunoreactive bands were visualized using enhanced chemiluminescence (ECL kit, Amersham) according to the manufacturer's instructions. Membranes were exposed to Biomax X-ray film (Kodak) for 30 s.

In vitro kinase activity assays

Cell extracts containing 100 μg of total protein were immunoprecipitated overnight with 5 μg of protein A-purified SIMK antibody. The immunoprecipitated kinase was washed three times with wash buffer (50 mM Tris–HCl pH 7.4, 250 mM NaCl, 5 mM EGTA, 0.1% Tween-20, 5 mM NaF) and once with kinase buffer (20 mM HEPES pH 7.4, 15 mM $MgCl_2$, 5 mM EGTA, 1 mM dithiothreitol). Kinase reactions were performed as described (Bögre *et al*., 1997). Briefly, the immunocomplexes were incubated for 30 min at room temperature in 15 μl of kinase buffer containing 1 mg/ml MBP, 0.1 mM ATP and 2 μCi of [γ-^{32}P]ATP. The reaction was stopped by adding SDS–PAGE loading buffer, and the phosphorylation of MBP was analyzed by autoradiography after SDS–PAGE.

Immunolocalization and microscopy

Immunolocalizations were performed using both freeze-shattering (Braun *et al*., 1999) and Steedman's wax embeding methods (Baluška *et al*., 2000a) except that half-strength stabilization buffer was used for sample fixation. Immunofluorescence images were collected using a Leica confocal microscope TCS4D (Leica, Heidelberg, Germany) or an Axioplan 2 microscope (Zeiss, Oberkochen, Germany).

Video microscopy of living root hairs

Video microscopy was performed as described by Foissner *et al*. (1996). Briefly, the brightfield image from an Univar microscope (Reichert-Leica, Austria) equipped with a 40× planapo objective was collected with a high-resolution video camera (Chalnicon C 1000.1, Hamamatsu, Germany), processed by a digital image processor (DVS 3000, Hamamatsu Germany) and recorded on digital video tape (JVC). Images and video scenes were imported into a personal computer (Sony Vaio).

Acknowledgements

We thank Markus Braun for his advice and help with freeze shattering. This work was supported by an EU Marie Curie individual fellowship to J.Š. and the EU Sokrates Program to A.H. Financial support to F.B. and D.V. by the Deutsches Zentrum für Luft- und Raumfahrt (Bonn, Germany) is highly appreciated. J.Š., J.S. and F.B. receive partial support from the Slovak Academy of Sciences, Grant Agency Vega (grants no. 2/6016/99 and 2031), Bratislava, Slovakia. We thank the Alexander von Humboldt foundation (Bonn, Germany) for donations of equipment. The work was also supported by grants to H.H. from the Austrian Science Foundation.

References

Baier,R., Schiene,K., Kohring,B., Flaschel,E. and Niehaus,K. (1999) Alfalfa and tobacco cells react differently to chitin oligosaccharides and *Sinorhizobium meliloti* nodulation factors. *Planta*, **210**, 157–164.

Baluška,F. and Volkmann,D. (2002) Actin-driven polar growth of plant cells. *Trends Cell Biol.*, **12**, 14.

Baluška,F., Salaj,J., Mathur,J., Braun,M., Jasper,F., Šamaj,J., Chua, N.-H., Barlow,P.W. and Volkmann,D. (2000a) Root hair formation: F-actin-dependent tip growth is initiated by local assembly of profilin-supported F-actin meshworks accumulated within expansin-enriched bulges. *Dev. Biol.*, **227**, 618–632.

Baluška,F., Ovecka,M. and Hirt,H. (2000b) Salt stress- and cell cycle phase-dependent changes in expression and subcellular localisation of the alfalfa mitogen-activated protein kinase SIMK. *Protoplasma*, **212**, 262–267.

Benndorf,R., Hayess,K., Ryazantsev,S., Wieske,M., Behlke,J. and Lutsch,G. (1994) Phosphorylation and supramolecular organization of murine small heat shock protein HSP25 abolish its actin polymerization-inhibiting activity. *J. Biol. Chem.*, **269**, 20780–20784.

Bibikova,T.N., Blancaflor,E.B. and Gilroy,S. (1999) Microtubules regulate tip growth and orientation in root hairs of *Arabidopsis thaliana*. *Plant J.*, **17**, 657–665.

Bögre,L., Ligterink,W., Meskiene,I., Barker,P.J., Heberle-Bors,E., Huskisson,N.S. and Hirt,H. (1997) Wounding induces the rapid and transient activation of a specific MAP kinase pathway. *Plant Cell*, **9**, 75–83.

Braun,M., Baluška,F., von Witsch,M. and Menzel,D. (1999) Redistribution of actin, profilin and phosphatidylinositol-4,5-bisphosphate (PIP_2) in growing and maturing root hairs. *Planta*, **209**, 435–443.

Brunner,D., Oellers,N., Szabad,J., Biggs,W.H., Zipursky,L.S. and Hafen,E. (1994) A gain of function mutation in *Drosophila* MAP kinase activates multiple receptor tyrosine kinase signaling pathways. *Cell*, **76**, 875–888.

Bubb,M.R., Spector,I., Beyer,B.B. and Fosen,K.M. (2000) Effects of jasplakinolide on the kinetics of actin polymerization. An explanation for certain *in vivo* observations. *J. Biol. Chem.*, **275**, 5163–5170.

Cardinale,F., Jonak,C., Ligterink,W., Niehaus,K., Boller,T. and Hirt,H. (2000) Differential activation of four specific MAPK pathways by distinct elicitors. *J. Biol. Chem.*, **275**, 36734–36740.

Chicurel,M.E., Chen,C.S. and Ingber,D.E. (1998) Cellular control lies in the balance of forces. *Curr. Opin. Cell Biol.*, **10**, 232–239.

Delley,P.-A. and Hall,M.N. (1999) Cell wall stress depolarizes cell growth via hyperactivation of RHO1. *J. Cell Biol.*, **147**, 163–174.

Diaz,C., Melchers,L., Hooykaas,P., Lugtenberg,B. and Kijne,J. (1989) Root lectin as a determinant of host-plant specificity in the *Rhizobium*–legume symbiosis. *Nature*, **338**, 579–581.

Fahraeus,G. (1957) The infection of clover root hairs by nodule bacteria studied by a simple glass slide technique. *J. Gen. Microbiol.*, **16**, 374–381.

Favata,M.F. *et al*. (1998) Identification of a novel inhibitor of mitogen-activated protein kinase kinase. *J. Biol. Chem.*, **273**, 18623–18632.

Ferrigno,P., Posas,F., Koepp,D., Saito,H. and Silver,P.A. (1998) Regulated nucleo/cytoplasmic exchange of HOG1 MAPK requires the importin b homologs NMD5 and XPO1. *EMBO J.*, **17**, 5606–5614.

Foissner,I., Lichtscheidl,I.K. and Wasteneys,G.O. (1996) Actin-based vesicle dynamics and exocytosis during wound wall formation in Characean internodal cells. *Cell Motil. Cytoskel.*, **35**, 35–48.

Fricker,W., Jarvis,M.C. and Brett,C.T. (2000) Turgor pressure, membrane tension and the control of exocytosis in higher plants. *Plant Cell Environ.*, **23**, 999–1003.

Gachet,Y., Tournier,S., Millar,J.B.A. and Hyams,J.S. (2001) A MAP kinase-dependent actin checkpoint ensures proper spindle orientation in fission yeast. *Nature*, **412**, 352–355.

Gibbon,B.C., Kovar,D.R. and Staiger,C.J. (1999) Latrunculin B has different effects on pollen germination and tube growth. *Plant Cell*, **11**, 2349–2363.

Hall,P.J., Cherkasova,V., Elion,E., Gustin,M.C. and Winter,E. (1996) The osmoregulatory pathway represses mating pathway activity in *Saccharomyces cerevisiae*: isolation of a FUS3 mutant that is insensitive to the repression mechanism. *Mol. Cell. Biol.*, **16**, 6715–6723.

Harrison,J.C., Bardes,E.S.G., Ohya,Y. and Lew,D.J. (2001) A role for the Pkc1p/Mpk1p kinase cascade in the morphogenesis checkpoint. *Nat. Cell Biol.*, **3**, 1–5.

Jiang,C.-J., Weeds,A.G. and Hussey,P.J. (1997) The maize actin-depolymerizing factor, ZmADF3, redistributes to the growing tip of elongating root hairs and can be induced to translocate into the nucleus with actin. *Plant J.*, **12**, 1035–1043.

Jonak,C., Kiegerl,S., Ligterink,W., Barker,P.J., Huskisson,N.S. and Hirt,H. (1996) Stress signaling in plants: a mitogen-activated protein kinase pathway is activated by cold and drought. *Proc. Natl Acad. Sci. USA*, **93**, 11274–11279.

Kamada,Y., Jung,U.S., Piotrowski,J. and Levin,D.E. (1995) The protein kinase C-activated MAP kinase pathway of *Saccharomyces cerevisiae* mediates a novel aspect of the heath shock response. *Genes Dev.*, **9**, 1559–1571.

Kell,A. and Glaser,R.W. (1993) On the mechanical and dynamic properties of plant cell membranes: their role in growth, direct gene transfer and protoplast fusion. *J. Theor. Biol.*, **160**, 41–62.

Kiegerl,S. *et al*. (2000) SIMKK, a mitogen-activated protein kinase (MAPK) kinase, is a specific activator of the salt stress-induced MAPK, SIMK. *Plant Cell*, **12**, 2247–2258.

Ko,K.S. and McCulloch,C.A.G. (2000) Partners in protection: interdependence of cytoskeleton and plasma membrane in adaptations to applied forces. *J. Membr. Biol.*, **174**, 85–95.

Leinweber,B.D., Leavis,P.C., Grabarek,Z., Wang,C.L.A. and Morgan,K.G. (1999) Extracellular regulated kinase (ERK) interaction with actin and the calponin homology (CH) domain of actin-binding proteins. *Biochem. J.*, **344**, 117–123.

Ligterink,W. and Hirt,H. (2001) Mitogen-activated protein (MAP) kinase pathways in plants: versatile signaling tools. *Int. Rev. Cytol.*, **201**, 209–215.

Ligterink,W., Kroj,T., zur Nieden,U., Hirt,H. and Scheel,D. (1997) Receptor-mediated activation of a MAP kinase in pathogen defense of plants. *Science*, **276**, 2054–2057.

Mazzoni,C., Zarzov,P., Rambourg,A. and Mann,C. (1993) The SLT2 (*MPK1*) MAP kinase homolog is involved in polarized cell growth in *Saccharomyces cerevisiae*. *J. Cell Biol.*, **123**, 1821–1833.

Miller,D.D., de Ruijter,N.C.A., Bisseling,T. and Emons,A.M.C. (1999) The role of actin in root hair morphogenesis: studies with lipochito-oligosaccharide as a growth stimulator and cytochalasin as an actin perturbing drug. *Plant J.*, **17**, 141–154.

Molendijk,A.J., Bischoff,F., Rajendrakumar,C.S.V., Friml,J., Braun,M., Gilroy,S. and Palme,K. (2001) *Arabidopsis thaliana* Rop GTPases are localized to tips of root hairs and control polar growth. *EMBO J.*, **20**, 2779–2788.

Munnik,T., Ligterink,W., Meskiene,I., Calderini,O., Beyerly,J., Musgrave,A. and Hirt,H. (1999) Distinct osmosensing protein kinase pathways are involved in signaling moderate and severe hyperosmotic stress. *Plant J.*, **20**, 381–388.

Nühse,T., Peck,S.C., Hirt,H. and Boller,T. (2000) Microbial elicitors induce activation and dual phosphorylation of the *Arabidopsis* MAP kinase AtMPK6. *J. Biol. Chem.*, **275**, 7521–7526.

Ovecka,M., Baluška,F., Nadubinská,M. and Volkmann,D. (2000) Actomyosin and exocytosis inhibitors alter root hair morphology in *Poa annua* L. *Biologia*, **55**, 105–114.

Robinson,M.J. and Cobb,M.H. (1997) Mitogen-activated protein kinase pathways. *Curr. Opin. Cell Biol.*, **9**, 180–186.

Robinson,M.J., Harkins,P.C., Zhang,J., Baer,R., Haycock,J.W., Cobb,M.H. and Goldsmith,E.J. (1996) Mutation of position 52 in ERK2 creates a nonproductive binding mode for adenosine 5′-triphosphate. *Biochemistry*, **35**, 5641–5646.

Rousseau,S., Houle,F., Landry,J. and Huot,J. (1997) p38 MAP kinase activation by vascular endothelial growth factor mediates actin reorganization and cell migration in human endothelial cells. *Oncogene*, **15**, 2169–2177.

Šamaj,J., Braun,M., Baluška,F., Ensikat,H.J., Tsumuraya,Y. and Volkmann,D. (1999) Specific localization of arabinogalactan–protein epitopes at the surface of maize root hairs. *Plant Cell Phys.*, **40**, 874–883.

Satiat-Jeunemaitre,B., Cole,L., Bourett,T., Howard,R. and Hawes,C. (1996) Brefeldin A effects in plant and fungal cells: something new about vesicle trafficking? *J. Microsc.*, **181**, 162–177.

Schäfer,C., Ross,S.E., Bragado,M.J., Groblewski,G.E., Ernst,S.A. and Williams,J.A. (1998) A role for the p38 mitogen-activated protein kinase/Hsp27 pathway in cholecystokinin-induced changes in the actin cytoskeleton in rat pancreatic acini. *J. Biol. Chem.*, **273**, 24173–24180.

Seo,S., Okamoto,M., Seto,H., Ishizuka,K., Sano,H. and Ohashi,Y. (1995) Tobacco MAP kinase: a possible mediator in wound signal transduction pathways. *Science*, **270**, 1988–1992.

Shaw,S.L., Dumais,J. and Long,S.R. (2000) Cell surface expansion in polarly growing root hairs of *Medicago truncatula*. *Plant Physiol.*, **124**, 959–969.

Sherrier,D.J. and VandenBosch,K.A. (1994) Secretion of cell wall polysaccharides in *Vicia* root hairs. *Plant J.*, **5**, 185–195.

Staiger,C.J. (2000) Signaling to the actin cytoskeleton in plants. *Annu. Rev. Plant Physiol. Plant Mol. Biol.*, **51**, 257–288.

Whitmarsh,A.J. and Davis,R.J. (1998) Structural organization of MAP-kinase signaling modules by scaffold proteins in yeast and mammals. *Trends Biochem. Sci.*, **23**, 481–485.

Wilson,C., Pfosser,M., Jonak,C., Hirt,H., Heberle-Bors,E. and Vicente,O. (1998) Evidence for the activation of a MAP kinase upon phosphate-induced cell cycle re-entry in tobacco cells. *Physiol. Plant.*, **102**, 532–538.

Woodring,P.J., Hunter,T. and Wang,J.Y.J. (2001) Inhibition of c-Abl tyrosine kinase activity by filamentous actin. *J. Biol. Chem.*, **276**, 27104–27110.

Zarzov,P., Mazzoni,C. and Mann,C. (1996) The SLT2 (MPK1) MAP kinase is activated during periods of polarized cell growth in yeast. *EMBO J.*, **15**, 83–91.

Zhang,S. and Klessig,D.F. (1998) The tobacco wounding-activated mitogen-activated protein kinase is encoded by SIPK. *Proc. Natl Acad. Sci. USA*, **95**, 7225–7230.

Received January 11, 2002; revised March 26, 2002; accepted May 14, 2002